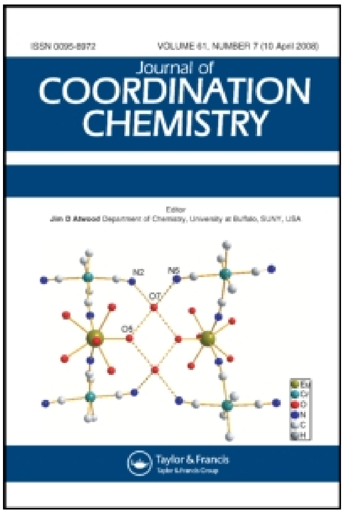

Journal of Coordination Chemistry
Publication details, including instructions for authors and subscription information:
http://www.informaworld.com/smpp/title~content=t713455674

Designed synthesis, structure, and 3-D topology of a supramolecular dimer and inorganic-organic cocrystal

Sujit Sasmal[a]; Susanta Hazra[a]; Sohini Sarkar[a]; Sasankasekhar Mohanta[a]
[a] Department of Chemistry, University of Calcutta, Kolkata 700 009, India

To cite this Article Sasmal, Sujit , Hazra, Susanta , Sarkar, Sohini and Mohanta, Sasankasekhar(2010) 'Designed synthesis, structure, and 3-D topology of a supramolecular dimer and inorganic-organic cocrystal', Journal of Coordination Chemistry, 63: 10, 1666 — 1677, First published on: 11 June 2010 (iFirst)

To link to this Article: DOI: 10.1080/00958972.2010.487939

URL: http://dx.doi.org/10.1080/00958972.2010.487939

Journal of Coordination Chemistry
Vol. 63, No. 10, 20 May 2010, 1666–1677

Taylor & Francis
Taylor & Francis Group

Designed synthesis, structure, and 3-D topology of a supramolecular dimer and inorganic–organic cocrystal

SUJIT SASMAL, SUSANTA HAZRA*, SOHINI SARKAR
and SASANKASEKHAR MOHANTA*

Department of Chemistry, University of Calcutta, 92 Acharya Prafulla
Chandra Road, Kolkata 700 009, India

(*Received 3 December 2009; in final form 29 January 2010*)

Synthesis and structure of a supramolecular dimer and inorganic–organic cocrystal of composition $[\{Cu^{II}L^1\subset(H_2O)\}_2(C_8H_6O_4)]$ (**1**) are described ($H_2L^1 = N,N'$-ethylenebis(3-ethoxysalicylaldimine); $C_8H_6O_4 =$ terephthalic acid). Crystal engineering has been utilized for the designed synthesis of the title compound. Compound **1** crystallizes in a triclinic system with $P\bar{1}$ space group. The structure consists of terephthalic acid and two symmetry related inclusion products $[Cu^{II}L^1\subset(H_2O)]$, in which the water molecule is encapsulated in the O_4 compartment by forming bifurcated hydrogen bonds involving two hydrogen of water and phenolate and ethoxy oxygens of the compartmental ligand. Hydrogen bonding between encapsulated water molecules and terephthalic acid forms the supramolecular dimer. The title compound is an example of an inorganic–organic cocrystal as well. Weak interactions, such as semicoordination of phenoxo oxygen of one unit to the metal center of a symmetry related unit and C–H $\cdots$ O, and O–H $\cdots$ O hydrogen bonds result in generation of an overall 3-D topology in the title compound. The 3-D topology can be understood as interlinking of two different 2-D sheets.

Keywords: Supramolecular; Inorganic–organic cocrystal; Terephthalic acid; 3-D; Inclusion compound

1. Introduction

Utilization of crystal engineering principles for self-assembly resulting from noncovalent interaction is a major focus of research in crystal engineering and supramolecular chemistry [1–12]. While self-assembly of organic molecules is now well explored, the same for aggregate containing metal complexes as a component is not yet an easy task.

Inclusion compounds or host–guest compounds are those in which a molecule (host) is the container of another molecule (guest) and the nature of attraction between the host and guest molecules are weak interactions, such as ion–dipole interactions, hydrogen bonding and $\pi \cdots \pi$ stacking [1, 2, 13–21]. Much research has been carried out

---

*Corresponding authors. Email: hazra_susanta1@yahoo.co.in; sm_cu_chem@yahoo.co.in

Journal of Coordination Chemistry
ISSN 0095-8972 print/ISSN 1029-0389 online
DOI: 10.1080/00958972.2010.487939

into the design and synthesis of inclusion compounds because of their potential for molecular recognition, separation, and catalysis [1].

Crystals may contain more than one species and these multicomponent crystals are known as cocrystals [20–46]. Organic cocrystals [22–38] are many in number and formation of these species can be explained on the basis of noncovalent interactions. In contrast, the cocrystals containing metal complexes [20, 21, 39–46] are comparatively less in number and the reason of cocrystallization in these aggregates is difficult to explain in most cases. Clearly, the design of cocrystals containing metal complexes as the components is not an easy task.

We have been exploring chemistry of mono-, di-, and oligonuclear complexes derived from compartmental Schiff-base ligands obtained on condensation of 3-ethoxysalicylaldehyde and diamines [19–21, 45–49]. Most of the mononuclear complexes derived from these ligands are host–guest or inclusion products in which a water molecule is encapsulated in the O_4 compartment by forming bifurcated hydrogen bonds involving water hydrogen and phenoxo and ethoxy oxygens [19–21, 45, 46]. The O_4 compartment is very good as a host for water as a guest that host–guest interaction also takes place in 3d–3d and 3d-alkali metal systems resulting in the formation of interesting examples of dinuclear–mononuclear cocrystals [20, 21, 45, 46]. We have been interested in whether it is possible to incorporate another host, e.g., dicarboxylic acid, in the O_4 cavity. In that case, two mononuclear complex units should be self-assembled to generate a dimer. Clearly, the desired compound if isolated will be an interesting example in the family of compounds (3d, 3d–4f, 3d–3d, 3d-main group, and 3d–5f), which we have been reporting. Another group has recently reported a dicarboxylic acid containing 3d compound in their attempt probably to synthesize a dicarboxylate bridged 3d–4f compound [50]. In this example, the dicarboxylic acid (naphthalene-2,6-dicarboxylic acid) is hydrogen bonded with encapsulated water. If dicarboxylic acid interacts with the O_4 cavity or with encapsulated water, the derived system will be a designed metal–organic cocrystal as well as a supramolecular dimer. The supramolecular structure may also be interesting because of the presence of another oxygen (C=O of carboxylic moiety). To check our anticipation, we have reacted the mononuclear inclusion product $[Cu^{II}L^1 \subset (H_2O)]$ with terephthalic acid ($H_2L^1 = N,N'$-ethylenebis(3-ethoxysalicylaldimine); scheme 1). We report in this investigation synthesis, characterization and molecular, and supramolecular structure of the product obtained therefrom.

2. Experimental

2.1. *Materials and physical measurements*

All reagents and solvents were purchased from commercial sources and used as received. The mononuclear inclusion product $[Cu^{II}L^1 \subset (H_2O)]$ was synthesized by the reported procedure [20]. Elemental (C, H, and N) analyses were performed on a Perkin Elmer 2400 II analyzer. IR spectra were recorded from 400 to 4000 cm^{-1} on a Bruker-Optics Alpha-T spectrophotometer with samples as KBr discs. Magnetic susceptibility measurements at 300 K were carried out with a Sherwood Scientific Co., UK magnetic susceptibility balance.

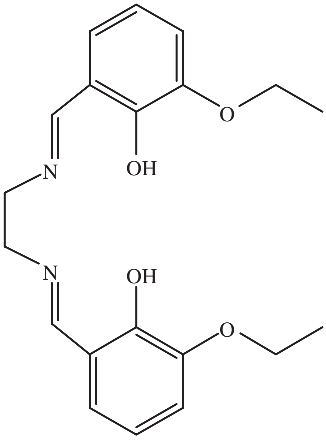

Scheme 1. Chemical structure of H_2L^1.

2.2. *Synthesis*

To a stirred suspension of $[Cu^{II}L^1 \subset (H_2O)]$ (0.110 g, 0.25 mmol) in methanol (50 mL) finely powdered terephthalic acid (0.332 g, 2 mmol) was added. After stirring for a few hours, the mixture was filtered to remove excess terephthalic acid and the clear filtrate was kept for slow evaporation. After 2 days, red crystalline compound containing diffractable single crystals deposited and were collected by filtration (yield 0.097 g, 75%). Selected FT-IR (KBr pellet (cm^{-1})): $\nu(H_2O)$, 3486(m), ν(OH), 2915(w), ν(C=O), 1695(m), ν(C=N), 1633(vs), ν(C–O), 1447(m). Anal. Calcd for $C_{48}H_{54}N_4O_{14}Cu_2$ (%): C, 55.54; H, 5.24; and N, 5.40. Found (%): C, 55.65; H, 5.10; and N, 5.35. μ_{eff}, 2.35 BM.

2.3. *Crystal structure determination*

The crystallographic data for **1** are summarized in table 1. Diffraction data were collected on a Bruker-APEX II SMART CCD diffractometer at 296 K using graphite-monochromated Mo-Kα radiation ($\lambda = 0.71073$ Å). For data processing and absorption correction, the packages SAINT [51] and SADABS [52] were used. The structure was solved by direct and Fourier methods and refined by full-matrix least-squares based on F^2 using SHELXTL [53] and SHELXL-97 [54]. All hydrogens were located from difference Fourier map. Using anisotropic treatment for the nonhydrogen atoms and isotropic treatment for the hydrogens, the final refinements converged at the R_1 values ($I > 2\sigma(I)$) 0.0299.

3. Results and discussion

3.1. *Description of the structure of* $[\{Cu^{II}L^1 \subset (H_2O)\}_2(C_8H_6O_4)]$ *(1)*

The crystal structure of **1** is shown in figure 1, while selected bond lengths and angles are listed in table 2. One half of the molecule of **1** is symmetry related to the other half.

Table 1. Crystallographic data for $[\{Cu^{II}L^1 \subset (H_2O)\}_2(C_8H_6O_4)]$ (**1**).

Empirical formula	$C_{48}H_{54}N_4O_{14}Cu_2$
Formula weight	1038.03
Temperature (K)	296(2)
Wavelength (Å)	0.71073
Crystal color	Red
Crystal system	Triclinic
Space group	$P\bar{1}$
Unit cell dimensions (Å, °)	
a	7.1003(5)
b	12.9037(9)
c	13.1368(9)
α	93.846(2)
β	96.344(2)
γ	105.734(2)
Volume (Å^3), Z	1145.46(14), 1
Calculated density (g cm^{-3})	1.505
Absorption coefficient (mm^{-1})	1.002
$F(000)$	540
θ range for data collection (°)	3.14–55.00
Reflections collected	15,547
Independent reflections	5079
Parameters	415
Goodness-of-fit on F^2	0.872
Final R indices $[I > 2\sigma(I)]$	$R_1{}^a = 0.0299$, $wR_2{}^b = 0.0976$
R indices (all data)	$R_1{}^a = 0.0373$, $wR_2{}^b = 0.1061$

$^aR_1 = [\sum ||F_o| - |F_c|| / \sum |F_o|]$; $^bwR_2 = [\sum w(F_o^2 - F_c^2)^2 / \sum wF_o^4]^{1/2}$.

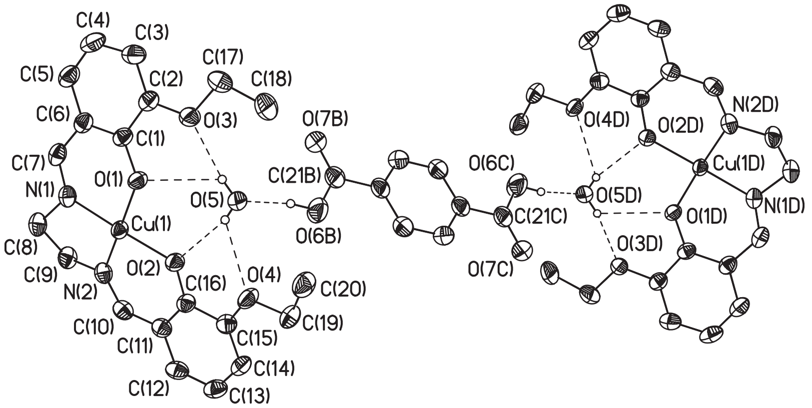

Figure 1. Crystal structure of $[\{Cu^{II}L^1 \subset (H_2O)\}_2(C_8H_6O_4)]$ (**1**). Hydrogens, except of water and CO_2H of terephthalic acid, are omitted for clarity. Symmetry code: B, $-1+x$, y, z; C, $-x$, $1-y$, $1-z$; and D, $-1-x$, $1-y$, $1-z$.

The crystal structure consists of two symmetry related inclusion products $[Cu^{II}L^1 \subset (H_2O)]$, which are interlinked due to O–H···O hydrogen bonds involving carboxylic O–H moiety of terephthalic acid as the donor and water oxygen as the acceptor. In $[Cu^{II}L^1 \subset (H_2O)]$, copper(II) occupies the N_2O_2 compartment, while the water molecule is encapsulated in the O_4 compartment by forming bifurcated hydrogen bonds involving two hydrogens of water and phenolate and ethoxy oxygens of the

Table 2. Selected bond lengths (Å) and angles (°) for **1**.

Cu(1)–N(1)	1.9394(16)
Cu(1)–N(2)	1.9431(16)
Cu(1)–O(1)	1.9265(13)
Cu(1)–O(2)	1.9106(13)
N(1)–Cu(1)–O(2)	174.04(6)
O(1)–Cu(1)–N(2)	174.05(6)
N(1)–Cu(1)–O(1)	92.77(6)
N(1)–Cu(1)–N(2)	84.36(7)
N(2)–Cu(1)–O(2)	93.04(6)
O(1)–Cu(1)–O(2)	89.32(6)

Table 3. Geometries (distances in (Å) and angles in (°)) of the hydrogen bonds in **1**.

D–H···A	D···A	H···A	D–H···A
O(5)–H(5A)···O(3)	2.845	2.114	162.1
O(5)–H(5A)···O(1)	2.914	2.435	122.5
O(5)–H(5B)···O(2)	2.752	2.121	159.8
O(5)–H(5B)···O(4)	2.816	2.358	128.3
O(6B)–H(6B)···O(5)	2.524	1.693	165.5
C(9)–H(9A)···O(1E)	3.468	2.558	158.3
C(3)–H(3)···O(7F)	3.377	2.584	165.1

Symmetry codes: A: $1-x$, $2-y$, $2-z$; B: $-1+x$, y, z; C: $-x$, $1-y$, $1-z$; D: $-1-x$, $1-y$, $1-z$; E: $-x$, $2-y$, $2-z$; and F: $1-x$, $1-y$, $2-z$.

compartmental ligand. The geometries of the four hydrogen bonds are listed in table 3. The donor···acceptor contacts in the range 2.75–2.91 Å can be considered as moderately strong. Similar moderately strong hydrogen bonds have been observed in the inclusion product [$Cu^{II}L^1\subset(H_2O)$] [19]. Deviation of the two phenoxo and two ethoxy oxygens from the least-squares O(phenoxo)$_2$O(ethoxy)$_2$ plane is 0.13 Å, indicating that these four oxygens of the larger ligand compartment may be considered an approximate plane. The water oxygen is displaced from this O_4 plane by 0.67 Å, indicating that the water is partially encapsulated in the O_4 compartment. In the mononuclear inclusion product [$Cu^{II}L^1\subset(H_2O)$], the water oxygen lies exactly in the least-squares O(phenoxo)$_2$O(ethoxy)$_2$ plane, perfectly encapsulated in the O_4 compartment. Evidently, the extent of water encapsulation in **1** is reduced due to the involvement of terephthalic acid to interlink the [$Cu^{II}L^1\subset(H_2O)$] moieties by forming terephthalic acid···water hydrogen bonds. Regarding the dinuclear–mononuclear cocrystals [$\{Cu^{II}L^1M^{II}(H_2O)_3\}\{Cu^{II}L^1\}_2$]($ClO_4$)$_2$, the oxygens of coordinated water that interact with the O_4 cavities are displaced by 0.92–1.23 Å from the least-squares O_4 plane [20]. Clearly, the extent of water encapsulation in these cocrystals is less than that in **1**. It is also evident, therefore, that steric factors to stabilize the crystalline phase in the title compound and in the dinuclear–mononuclear cocrystals are the reasons for partial encapsulation of water in these cases.

As already mentioned, two symmetry related [$Cu^{II}L^1\subset(H_2O)$] moieties in **1** are interlinked due to terephthalic acid···water hydrogen bond in which former is the donor and the latter is the acceptor. The geometry of this hydrogen bond (O(6B)–H(6B)···O(5); figure 1; B, $-1+x$, y, z) is listed in table 3. As the donor $\cdots$ acceptor contact is 2.524 Å, this hydrogen bond should be considered as a strong interaction. Clearly, the interaction between terephthalic acid and O_4 cavity does not take place and therefore the former is not a guest for $[Cu^{II}L^1]$ to make a self-assembly. However, water acts as a guest in the O_4 cavity and the formation of hydrogen bonds between terephthalic acid and that encapsulated water results in the dimeric self-assembly in the title compound. Clearly, the dicarboxylic acid here acts as a supramolecular synthon and the dimeric self-assembly $[\{Cu^{II}L^1{\subset}(H_2O)\}_2(C_8H_6O_4)]$ (**1**) is a supramolecular dimer. Again, as two $[Cu^{II}L^1{\subset}(H_2O)]$ moieties and one terephthalic acid exist in a single crystal due to their interlinking by noncovalent interactions, the title compound is an example of cocrystal of metal complex units and an organic moiety.

While one mononuclear unit, $[Cu^{II}L^1{\subset}(H_2O)]$, is interlinked with a neighboring symmetry related unit, $[Cu^{II}(1D)L^1{\subset}(H_2O)]$ (D, $-1-x$, $1-y$, $1-z$) by terephthalic acid (figure 1), $[Cu^{II}L^1{\subset}(H_2O)]$ is also interlinked with another symmetry related unit, $[Cu^{II}(1A)L^1{\subset}(H_2O)]$ (A, $1-x$, $2-y$, $2-z$) due to semicoordination of one phenoxo oxygen (O(2)) to the metal center (Cu(1A)) of the adjacent molecule (figure 2). Clearly, the mononuclear $[Cu^{II}L^1{\subset}(H_2O)]$ units in **1** are self-assembled to dimeric species due to this semicoordination. The Cu(1)–O(1A) distance is 2.589 Å and the bond angles involving O(1A), Cu(1) and each of the four atoms (N(1), N(2), O(1), and O(2)), coordinated to Cu(1), lie in the range 89.31–96.00°. Clearly, considering the semicoordination of O(1A) to Cu(1), the coordination geometry of the metal center in **1** can be described as pseudo-square pyramidal with a phenoxo oxygen (O(1A)) as the apical atom and the N_2O_2 compartment of ligand forming the basal plane. The N_2O_2 donors of this plane form a perfect plane from which the copper(II) ion is displaced by only 0.09 Å. Both Cu–N bond distances in **1** are identical (Cu(1)–N(1) = 1.9394(16) Å; Cu(1)–N(2) = 1.9431(16) Å) within experimental error, as are the Cu–O bond lengths (Cu(1)–O(1) = 1.9265(13) Å; Cu(1)–O(2) = 1.9106(13) Å) and the Cu–N(imine) bond distances are slightly longer than the Cu–O(phenoxo) bond lengths. While the *transoid* angles in **1** (174.04(6)° and 174.05(6)°) are equal, the *cisoid* angles lie in the

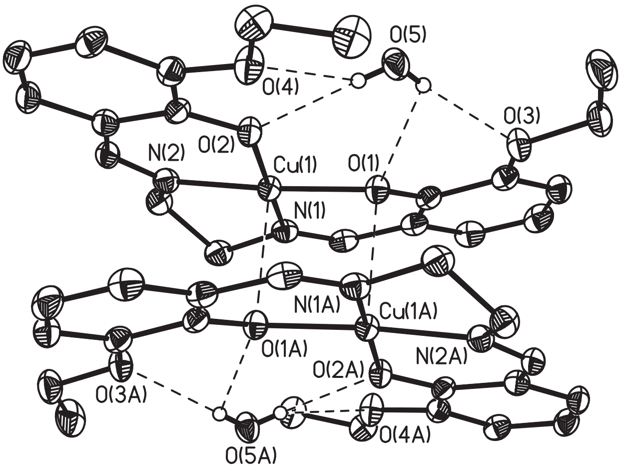

Figure 2. Perspective view to show the interlinking of two symmetry related $[Cu^{II}L^1{\subset}(H_2O)]$ units in $[\{Cu^{II}L^1{\subset}(H_2O)\}_2(C_8H_6O_4)]$ (**1**) due to semicoordination of phenoxo oxygen. Terephthalic acid is omitted for clarity. Hydrogens, except of water, are omitted for clarity. Symmetry code: A: $1-x$, $2-y$, $2-z$.

range 84.36(7)–93.04(6)°, indicating only little deviation of the coordination geometry of Cu(II).

The overall supramolecular topology of the title compound is 3-D, which can be better understood by presenting the analysis as different fragments. As shown in figure 3, the supramolecular structure of **1** excluding terephthalic acid is 1-D. In this case, the dimer resulting from phenoxo $\cdots$ copper(II) semicoordination is self-assembled due to a weak C–H $\cdots$ O hydrogen bond involving one hydrogen (H(9A)) linked with the carbon (C(9)) of lateral diimino side chain and the phenoxo oxygen O(1E; E, $-x$, $2-y$, $2-z$). For convenience, we designate this 1-D chain as Chain 1. As already mentioned, O(6B)–H(6B) $\cdots$ O(5) hydrogen bond involving terephthalic acid and encapsulated water results in the formation of supramolecular dimer. As shown in figure 4, this hydrogen bond also interlinks the adjacent 1-D topologies (Chain 1) to generate a 2-D sheet (Sheet 1). The 1-D topologies (Chain 1) are also interlinked to develop another 2-D sheet (Sheet 2; figure 5) due to another hydrogen bond (C(3)–H(3) $\cdots$ O(7F); F, $1-x$, $1-y$, $2-z$) involving C=O of terephthalic acid as the acceptor and a C–H moiety as the donor (figure S1, Supplementary material). The overall 3-D topology of the title compound can therefore be demonstrated in terms of these two interlinked 2-D sheets (Sheets 1 and 2; figure 6). Clearly, one terephthalic acid molecule is surrounded by four different symmetry related $[\mathrm{Cu^{II}L^1}\subset(\mathrm{H_2O})]$ dimers through O(6B)–H(6B) $\cdots$ O(5) and C(3)–H(3) $\cdots$ O(7F) interactions (figure S2, Supplementary material). Space-filling diagrams along the three crystallographic axes are demonstrated in figure 7; space created by $[\mathrm{Cu^{II}L^1}\subset(\mathrm{H_2O})]$ moieties is occupied by terephthalic acid.

3.2. *Synthesis and characterization*

The reaction between the mononuclear inclusion compound $[\mathrm{Cu^{II}L^1}\subset(\mathrm{H_2O})]$ and terephthalic acid produces the red crystalline compound $[\{\mathrm{Cu^{II}L^1}\subset(\mathrm{H_2O})\}_2(\mathrm{C_8H_6O_4})]$ (**1**).

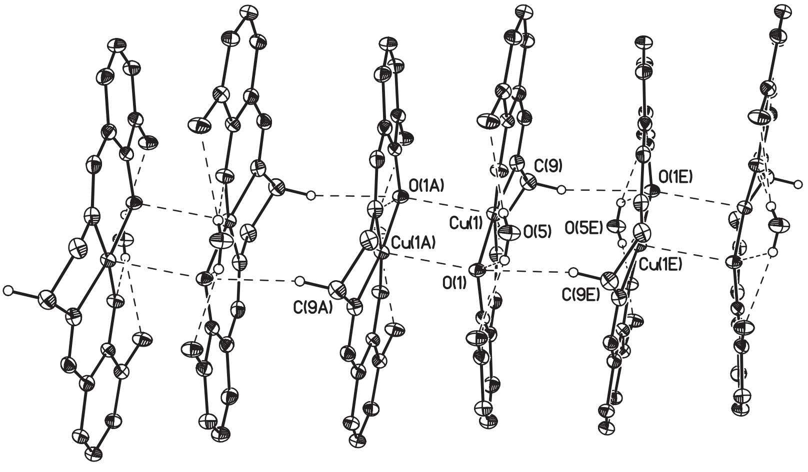

Figure 3. Perspective view to show the interlinking of the dimer in figure 2 due to C(9)–H(9A) $\cdots$ O(1E) interaction to generate a 1-D chain (Chain 1). Ethoxy carbons, terephthalic acid, and hydrogens, except those participating in H-bonds, are omitted for clarity. Symmetry codes: A: $1-x$, $2-y$, $2-z$; and E: $-x$, $2-y$, $2-z$.

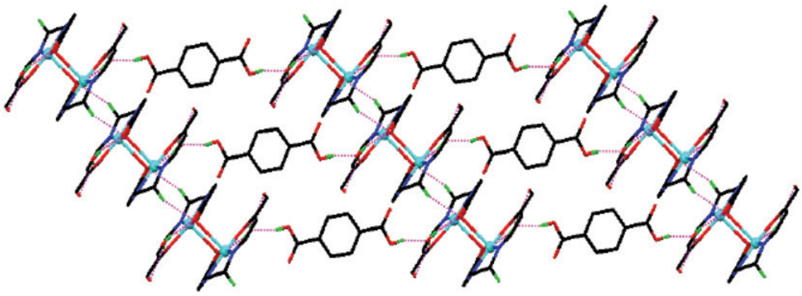

Figure 4. Presentation of the 2-D sheet (Sheet 1), down the crystallographic *b*-axis, resulting from O(6B)–H(6B) $\cdots$ O(5) interaction among the 1-D chains (in figure 3). Several atoms are omitted for clarity. Symmetry code: B: $-1+x$, y, z.

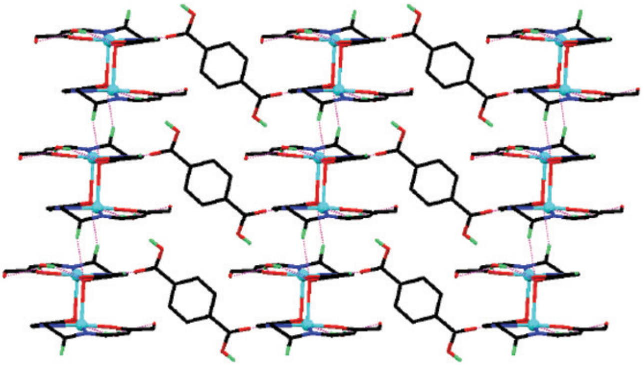

Figure 5. Presentation of the 2-D sheet (Sheet 2) down the crystallographic *b*-axis, generated due to the C(3)–H(3) $\cdots$ O(7F) interaction among the 1-D chains (in figure 3). Several atoms are omitted for clarity. Symmetry code: F: $1-x$, $1-y$, $2-z$.

In comparison to the imine stretching of $[Cu^{II}L^1\subset(H_2O)]$ at $1620\,cm^{-1}$ [20], the vibration due to $\nu_{C=N}$ appears at slightly higher energy ($1633\,cm^{-1}$) for **1**. One medium intensity band at $1695\,cm^{-1}$ may be assigned for C=O group. The water stretches appear as a medium intensity band at $3486\,cm^{-1}$. Symmetric and antisymmetric stretches of encapsulated water in $[Cu^{II}L^1\subset(H_2O)]$ appear separately at 3518 and $3568\,cm^{-1}$, respectively [20]. While water molecule in $[Cu^{II}L^1\subset(H_2O)]$ is perfectly encapsulated, the extent of encapsulation of the water molecule in $[\{Cu^{II}L^1\subset(H_2O)\}_2(C_8H_6O_4)]$ (**1**) is much less. Therefore, as restriction on vibration of water in **1** is less, the two stretches are not separate.

The room temperature (300 K) magnetic moment (2.35 BM) of **1** is slightly less than the spin-only value (2.45 BM) expected for the two isolated copper(II) centers. The magnetic exchange interactions in dinuclear, oligonuclear, and polymeric copper(II) complexes have been extensively investigated. Several magneto-structural correlations have also been determined [55–69]. The magnetic orbital for a copper(II) is $d_{x^2-y^2}$. If the diamagnetic bridging atom occupies equatorial positions of the coordination environments of both the copper(II) centers (equatorial–equatorial combination), the magnetic exchange interaction between the two $d_{x^2-y^2}$ orbitals through the orbital of the diamagnetic bridging atom becomes more efficient [55–60]. In that case, the interaction

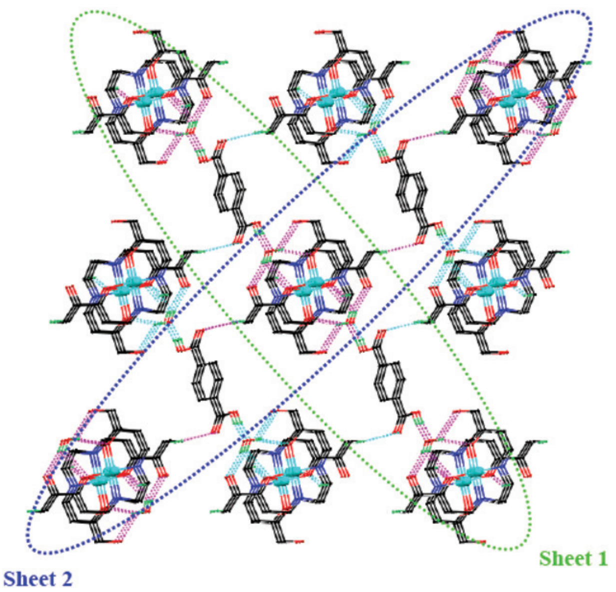

Figure 6. Illustration of the 3-D topology down the crystallographic *a*-axis from interlinking of the two 2-D sheets (Sheet 1 in figure 4 and Sheet 2 in figure 5).

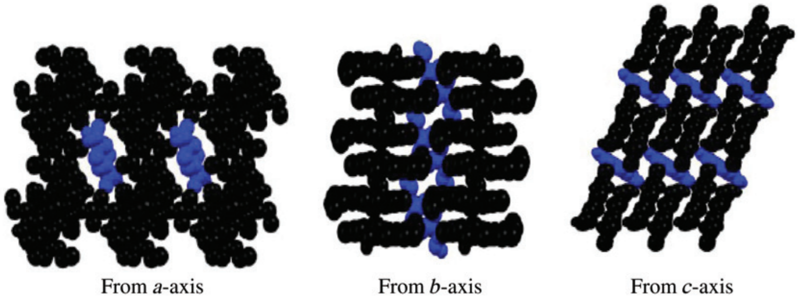

Figure 7. Space-filling packing diagram of $[\{Cu^{II}L^1\subset(H_2O)\}_2(C_8H_6O_4)]$ (**1**). Blue and black colors represent terephthalic acid and $[Cu^{II}L^1\subset(H_2O)]$ units, respectively.

is stronger if the bridge angle is larger, while accidental orthogonality assisted ferromagnetic interaction takes place for smaller bridge angles. On the other hand, if the bridging atom occupies axial positions of the two metal centers (axial–axial combination), $d_{x^2-y^2}$ orbitals will not be directed toward the bridge resulting in practically negligible magnetic exchange interaction. Again, if the bridging atom occupies an equatorial position of one metal center and an axial position of the second metal center (equatorial–axial combination), $d_{x^2-y^2}$ of one metal ion and d_{z^2} of the second metal ion will be directed toward the bridge [64–68]. The metal centers interact only weakly in this equatorial–axial combination if the bridging atoms form efficient bonding with both the metal ions. On the other hand, if one of the two metal–ligand (bridging) bonds is weak enough for equatorial–axial combination, the possibility of interaction should be further diminished. In **1**, mononuclear copper(II) moieties are self-assembled due to weak interactions, five O–H ··· O and two C–H ··· O hydrogen bonds and Cu ··· O(phenoxo) semicoordination. Among these, the five O–H ··· O hydrogen bonds interlink two mononuclear moieties through terephthalic acid and encapsulated water molecules (figure 1). The distance between the metal centers of the mononuclear units interlinked by the five O–H ··· O hydrogen bonds is very long (18.16 Å) as well. Clearly, it is logical to conclude that the five O–H ··· O hydrogen bonds cannot mediate magnetic exchange interaction. It is also logical to consider that two weak C–H ··· O hydrogen bonds (figures 3 and 5) do not propagate magnetic exchange. The only possible pathway of magnetic interaction may be therefore the Cu ··· O(phenoxo) pathway (figure 2). The bridging phenoxo oxygen occupies equatorial position of one metal center and axial position of the second metal center. Therefore, as already discussed, magnetic exchange interaction for this equatorial–axial combination should be very small. Again, although the bridging phenoxo oxygen is coordinated to one copper(II) center, Cu(1)–O(1) = 1.9265(13) Å, the interaction of the phenoxo oxygen with the second copper(II) ion is just semicoordination, Cu(1A) ··· O(1) = 2.589 Å. Clearly, the possibility of magnetic exchange interaction is further diminished due to this semicoordination. In brief, due to equatorial–axial combination and also due to semicoordination of the bridging atom to a metal center, the magnetic exchange interaction through the phenoxo bridging moiety should be only very weak. The room temperature magnetic moment, 2.35 BM, of **1** is only slightly less than the theoretical value of isolated spin combination, which indicates that the metal centers in **1** are probably coupled by very weak antiferromagnetic interaction.

4. Conclusions

Of the dinuclear–mononuclear cocrystals, $[\{Cu^{II}L^1\subset(H_2O)\}_2(C_8H_6O_4)]$ (**1**) is another example that exhibits the strong tendency of water to encapsulate in the $O(phenoxo)_2O(ethoxy)_2$ cavity. Although water is not replaced by terephthalic acid as a guest, the terephthalic acid ··· water interaction results in the formation of a supramolecular dimer and metal–organic cocrystal. Clearly, crystal engineering has been utilized here for the synthesis of a self-assembly. Moreover, the combined effect of weak interactions results in the generation of 3-D supramolecular topology in the title compound. Therefore, this investigation is an interesting addition in the area of supramolecular chemistry.

Supplementary material

Figure S1 is for the illustration of C(3)–H(3) ··· O(7F) interaction, which connects the two mononuclear moieties by terephthalic acid and figure S2 for the illustration of the interlinking of one terephthalic acid molecule with four different mononuclear units. Crystallographic information are available (CCDC reference no. 746397) from the Cambridge Crystallographic Data Center, 12 Union Road, Cambridge CB2 1EZ, UK (Fax: +44 1223 336 033; Email: deposit@ccdc.cam.ac.uk).

Acknowledgments

Financial support from the Department of Science and Technology, the Government of India (SR/S1/IC-12/2008), Council for Scientific and Industrial Research (Fellowship to S. Hazra) and University Grant Commission (Fellowship to S. Sasmal and S. Sarkar) are acknowledged.

References

[1] J.L. Atwood, J.E.D. Devies, D.D. MacNicol (Eds). *Inclusion Compounds*, Vol. 1–3, Academic Press, London (1984).

[2] J.L. Atwood, J.E.D. Devies, D.D. MacNicol, F. Vögtle, J.-M. Lehn, G.W. Gokel (Eds). *Comprehensive Supramolecular Chemistry*, Vol. 1, Pergamon Press, Exeter, UK (1996).

[3] G.R. Desiraju (Ed.). *The Crystal as a Supramolecular Entity Perspectives in Supramolecular Chemistry*, Vol. 2, Wiley, London (1996).

[4] D. Braga, F. Grepioni, A.G. Orpen. *Crystal Engineering: from Molecules and Crystals to Materials*, Kluwer Academic, Dordrecht, The Netherlands (1999).

[5] D. Braga, L. Maini, M. Polito, L. Scaccianoce, G. Cojazzi, F. Grepioni. *Coord. Chem. Rev.*, **216–217**, 225 (2001).

[6] B. Moulton, M.J. Zaworotko. *Chem. Rev.*, **101**, 1629 (2001).

[7] K.I. Nättinen, K. Rissanen. *Cryst. Eng. Commun.*, **5**, 326 (2003).

[8] D. Braga, S.L. Giaffreda, F. Grepioni, L. Maini, M. Polito. *Coord. Chem. Rev.*, **250**, 1267 (2006).

[9] R. Robson. In *Comprehensive Supramolecular Chemistry*, J.L. Atwood, J.E.D. Devies, D.D. MacNicol, F. Vögtle, R.B. Toda (Eds), Vol. 6, p. 733, Pergamon, Oxford, UK (1996).

[10] R. Koner, M. Nayak, G. Ferguson, J.N. Low, C. Glidewell, P. Misra, S. Mohanta. *Cryst. Eng. Commun.*, **7**, 129 (2005).

[11] S. Hazra, S. Majumder, M. Fleck, N. Aliaga-Alcalde, S. Mohanta. *Polyhedron*, **28**, 3707 (2009).

[12] M. Nayak, R. Koner, H. Stoeckli-Evans, S. Mohanta. *Cryst. Growth Des.*, **5**, 1907 (2005).

[13] G. Hoshina, S. Ohba, K. Nakajima, H. Ishida, M. Kojima, M. Tsuchimoto. *Bull. Chem. Soc. Japan*, **72**, 1037 (1999).

[14] G. Hoshina, M. Tsuchimoto, S. Ohba, K. Nakajima, H. Vekusa, Y. Ohashi, H. Ishida, M. Kojima. *Inorg. Chem.*, **37**, 142 (1998).

[15] R. Kasahara, M. Tsuchimoto, S. Ohba, K. Nakajima, H. Ishida, M. Kojima. *Inorg. Chem.*, **35**, 7661 (1996).

[16] J.R. Zamian, E.R. Dockal, G. Castellano, G. Olive. *Polyhedron*, **14**, 2411 (1995).

[17] B. Jing, L. Li, D. Wang, T. Xu, X. Guo. *Acta Cryst.*, **E61**, m2244 (2005).

[18] H. Schmidt, D. Rehder. *Inorg. Chim. Acta*, **267**, 229 (1998).

[19] S. Hazra, R. Koner, M. Nayak, H.A. Sparkes, J.A.K. Howard, S. Dutta, S. Mohanta. *Eur. J. Inorg. Chem.*, 4887 (2009).

[20] M. Nayak, R. Koner, H.-H. Lin, U. Flörke, H.-H. Wei, S. Mohanta. *Inorg. Chem.*, **45**, 10764 (2006).

[21] M. Nayak, S. Hazra, P. Lemoine, R. Koner, C.R. Lucas, S. Mohanta. *Polyhedron*, **27**, 1201 (2008).

[22] J.F. Remenar, S.L. Morissette, M.L. Peterson, B. Moulton, J.M. MacPhee, H.R. Guzman, O. Almarsson. *J. Am. Chem. Soc.*, **125**, 8456 (2003).

[23] T.E. Keyes, R.J. Forster, A.M. Bond, W. Miao. *J. Am. Chem. Soc.*, **123**, 2877 (2001).

[24] H. Koshima, H. Miyamoto, I. Yagi, K. Uosaki. *Cryst. Growth Des.*, **4**, 807 (2004).

[25] P.L. Magueres, S.M. Hubig, S.V. Lindeman, P. Veya, J.K. Kochi. *J. Am. Chem. Soc.*, **122**, 10073 (2000).

[26] B. Sarma, L.S. Reddy, A. Nangia. *Cryst. Growth Des.*, **8**, 4546 (2008).

[27] Z. Deutsch, J. Bernstein. *Cryst. Growth Des.*, **8**, 3537 (2008).

[28] J.A. Bis, O.L. McLaughlin, P. Vishweshwar, M.J. Zaworotko. *Cryst. Growth Des.*, **6**, 2648 (2006).

[29] G.P. Stahly. *Cryst. Growth Des.*, **7**, 1007 (2007).

[30] S. Karki, L. Fábián, T. Friščić, W. Jones. *Org. Lett.*, **9**, 3133 (2007).

[31] F.G. Vogt, J.S. Clawson, M. Strohmeier, A.J. Edwards, T.N. Pham, S.A. Watson. *Cryst. Growth Des.*, **9**, 921 (2009).

[32] W.-H. Wang, P.-H. Xi, X.-Y. Su, J.-B. Lan, Z.-H. Mao, J.-S. You, R.-G. Xie. *Cryst. Growth Des.*, **7**, 741 (2007).

[33] L.R. MacGillivray, G.S. Papaefstathiou, T. Friščić, T.D. Hamilton, D.-K. Bučar, Q. Chu, D.B. Varshney, I.G. Georgiev. *Acc. Chem. Res.*, **41**, 280 (2008).

[34] N. Takata, K. Shiraki, R. Takano, Y. Hayashi, K. Terada. *Cryst. Growth Des.*, **8**, 3032 (2008).

[35] H. Koshima, M. Nagano, T. Asahi. *J. Am. Chem. Soc.*, **127**, 2455 (2005).
[36] S.L. Childs, L.J. Chyall, J.T. Dunlap, V.N. Smolenskaya, B.C. Stahly, G.P. Stahly. *J. Am. Chem. Soc.*, **126**, 13335 (2004).
[37] F. Pan, M.S. Wong, V. Gramlich, C. Bosshard, P. Gunter. *J. Am. Chem. Soc.*, **118**, 6315 (1996).
[38] S. Mohamed, D.A. Tocher, M. Vickers, P.G. Karamertzanis, S.L. Price. *Cryst. Growth Des.*, **9**, 2881 (2009).
[39] C.-C. Chou, C.-C. Su, H.-L. Tsai, K.-H. Lii. *Inorg. Chem.*, **44**, 628 (2005).
[40] M. Palaniandavar, R.J. Butcher, A.W. Addison. *Inorg. Chem.*, **35**, 467 (1996).
[41] R.C. Holz, L.C. Thompson. *Inorg. Chem.*, **32**, 5251 (1993).
[42] P. Jones, R.S. Vagg, P.A. Williams. *Inorg. Chem.*, **23**, 4110 (1984).
[43] W.J. Evans, T.J. Boyle, J.W. Ziller. *Inorg. Chem.*, **31**, 1120 (1992).
[44] P.J. Dyson, J.W. Steed, P. Suman. *Cryst. Eng. Commun.*, **1**, 5 (1999).
[45] S. Hazra, S. Sasmal, M. Nayak, H.A. Sparkes, J.A.K. Howard, S. Mohanta. *Cryst. Eng. Commun.*, **12**, 470 (2010).
[46] S. Hazra, R. Koner, M. Nayak, H.A. Sparkes, J.A.K. Howard, S. Mohanta. *Cryst. Growth Des.*, **9**, 3603 (2009).
[47] S. Mohanta, H.-H. Lin, C.-J. Lee, H.-H. Wei. *Inorg. Chem. Commun.*, **5**, 585 (2002).
[48] R. Koner, H.-H. Lin, H.-H. Wei, S. Mohanta. *Inorg. Chem.*, **44**, 3524 (2005).
[49] R. Koner, G.-H. Lee, Y. Wang, H.-H. Wei, S. Mohanta. *Eur. J. Inorg. Chem.*, 1500 (2005).
[50] E.C. Constable, G. Zhang, C.E. Housecroft, M. Neuburger, S. Schaffner. *Cryst. Eng. Commun.*, **11**, 657 (2009).
[51] Bruker–Nonius. *APEX-II*, *SAINT-Plus and TWINABS*, Bruker–Nonius AXS Inc., Madison, Wisconsin, USA (2004).
[52] G.M. Sheldrick. *SAINT* (*Version 6.02*), *SADABS* (*Version 2.03*), Bruker AXS Inc., Madison, Wisconsin, USA (2002).
[53] G.M. Sheldrick. *SHELXTL* (*Version 6.10*), Bruker AXS Inc., Madison, Wisconsin, USA (2002).
[54] G.M. Sheldrick. *SHELXL-97*, *Crystal Structure Refinement Program*, University of Göttingen, Germany (1997).
[55] O. Kahn. *Molecular Magnetism*, VCH Publications, New York (1993).
[56] V.M. Crawford, M.W. Richardson, J.R. Wasson, D.J. Hodgson, W.E. Hatfield. *Inorg. Chem.*, **15**, 2107 (1976).
[57] M. Handa, N. Koga, S. Kida. *Bull. Chem. Soc. Japan*, **61**, 3853 (1988).
[58] L. Merz, W. Haase. *J. Chem. Soc., Dalton Trans.*, 875 (1980).
[59] L.K. Thompson, S.K. Mandal, S.K. Tandon, J.N. Bridson, M.K. Park. *Inorg. Chem.*, **35**, 3117 (1996).
[60] Y.-M. Sun, P.-G. Li, J.-M. Shi. *J. Coord. Chem.*, **62**, 1725 (2009).
[61] Y.-C. Chou, S.-F. Huang, R. Koner, G.-H. Lee, Y. Wang, S. Mohanta, H.-H. Wei. *Inorg. Chem.*, **43**, 2759 (2004).
[62] S. Majumder, R. Koner, P. Lemoine, M. Nayak, M. Ghosh, S. Hazra, R.C. Lucas, S. Mohanta. *Eur. J. Inorg. Chem.*, 3447 (2009).
[63] S.R. Batten, K.S. Murray. *Coord. Chem. Rev.*, **246**, 103 (2003).
[64] J.-M. Li, X. Jin. *J. Coord. Chem.*, **62**, 2610 (2009).
[65] B. Vangdal, J. Carranza, F. Lloret, M. Julve, J. Sletten. *J. Chem. Soc., Dalton Trans.*, 566 (2002).
[66] M. Du, X.-J. Zhao, S.R. Batten, J. Ribas. *Cryst. Growth Des.*, **5**, 901 (2005).
[67] P. Mishra, C.-Y. Liao, H.-H. Wei, S. Mohanta. *Polyhedron*, **27**, 1185 (2008).
[68] Y.-Y. Kou, J.-L. Tian, D.-D. Li, H. Liu, W. Gu, S.-P. Yan. *J. Coord. Chem.*, **62**, 2182 (2009).
[69] S.N. Herringer, M.M. Turnbull, C.P. Landee, J.L. Wikaira. *J. Coord. Chem.*, **62**, 863 (2009).